Title

Inhibition of galectin-3 post-infarction impedes progressive fibrosis by regulating inflammatory profibrotic cascades.

Journal

Cardioscience, 119(15)

Authors

Wang, Xiaoyin
Gaur, Meenakshi
Mounzih, Khalid
et al.

Publication Date

2023-11-25

DOI

10.1093/cvr/cvad116

Peer reviewed

ESC European Society of Cardiology

Cardiovascular Research (2023) **119**, 2536–2549
https://doi.org/10.1093/cvr/cvad116

Inhibition of galectin-3 post-infarction impedes progressive fibrosis by regulating inflammatory profibrotic cascades

Xiaoyin Wang [1,2†], Meenakshi Gaur[3†‡], Khalid Mounzih[3], Hilda J. Rodriguez[1,2,3], Huiliang Qiu[1,2¶], Ming Chen[1§], Liqiu Yan[1‖], Brian A. Cooper[3#], Shilpa Narayan[1,2], Ronak Derakhshandeh[1,2], Poonam Rao[1,2††], Daniel D. Han[1‡‡], Pooneh Nabavizadeh[2¶¶], Matthew L. Springer [1,2]*, and Constance M. John [3,4]***

[1]Division of Cardiology, University of California, San Francisco, 505 Parnassus Avenue, San Francisco, CA 94143, USA; [2]Cardiovascular Research Institute, University of California, San Francisco, 555 Mission Bay Boulevard South, San Francisco, CA 94158, USA; [3]MandalMed, Inc., 665 3rd Street, Suite 250, San Francisco, CA 94107, USA; and [4]Department of Laboratory Medicine, University of California, San Francisco, 185 Berry Street, Suite 100, San Francisco, CA 94143, USA

Received 27 July 2022; revised 2 April 2023; accepted 12 May 2023; online publish-ahead-of-print 21 August 2023

Time of primary review: 35 days

See the editorial comment for this article 'Targeting galectin-3 in myocardial infarction: a unique opportunity for biomarker-guided therapy', by N.G. Frangogiannis, https://doi.org/10.1093/cvr/cvad156.

Aims Acute myocardial infarction (MI) causes inflammation, collagen deposition, and reparative fibrosis in response to myocyte death and, subsequently, a pathological myocardial remodelling process characterized by excessive interstitial fibrosis, driving heart failure (HF). Nonetheless, how or when to limit excessive fibrosis for therapeutic purposes remains uncertain. Galectin-3, a major mediator of organ fibrosis, promotes cardiac fibrosis and remodelling. We performed a preclinical assessment of a protein inhibitor of galectin-3 (its C-terminal domain, Gal-3C) to limit excessive fibrosis resulting from MI and prevent ventricular enlargement and HF.

Methods and results Gal-3C was produced by enzymatic cleavage of full-length galectin-3 or by direct expression of the truncated form in *Escherichia coli*. Gal-3C was intravenously administered for 7 days in acute MI models of young and aged rats, starting either pre-MI or 4 days post-MI. Echocardiography, haemodynamics, histology, and molecular and cellular analyses were performed to assess post-MI cardiac functionality and pathological fibrotic progression. Gal-3C profoundly benefitted left ventricular ejection fraction, end-systolic and end-diastolic volumes, haemodynamic parameters, infarct scar size, and interstitial fibrosis, with better therapeutic efficacy than losartan and spironolactone monotherapies over the 56-day study. Gal-3C therapy in post-MI aged rats substantially improved pump function and attenuated ventricular dilation, preventing progressive HF. Gal-3C *in vitro* treatment of M2-polarized macrophage-like cells reduced their M2-phenotypic expression of arginase-1 and interleukin-10. Gal-3C inhibited M2 polarization of cardiac macrophages during reparative response post-MI. Gal-3C impeded progressive fibrosis post-MI by down-regulating galectin-3-mediated profibrotic signalling cascades including a reduction in endogenous arginase-1 and inducible nitric oxide synthase (iNOS).

Conclusion Gal-3C treatment improved long-term cardiac function post-MI by reduction in the wound-healing response, and inhibition of inflammatory fibrogenic signalling to avert an augmentation of fibrosis in the periinfarct region. Thus, Gal-3C treatment prevented the infarcted heart from extensive fibrosis that accelerates the development of HF, providing a potential targeted therapy.

* Corresponding author. Tel: +1 415 495 5570, E-mail: connie@mandalmed.com (C.M.J.); Tel: +1 415 502 8404; fax: +1 415 476 9802, E-mail: matt.springer@ucsf.edu (M.L.S.)
† These authors contributed equally to the study.
‡ Present address. Aelan Cell Technologies, San Francisco, CA, USA.
¶ Present address. Department of Cardiovascular Diseases, Physiology and Biomedical Engineering, Mayo Clinic Arizona, Scottsdale, AZ, USA.
§ Present address. Department of Cardiology, Zhongnan Hospital of Wuhan University, Wuhan, China.
‖ Present address. Department of Cardiology, Cangzhou Central Hospital, Cangzhou, Hebei, China.
Present address. Department of Biology, Massachusetts Institute of Technology, Cambridge, MA, USA.
** Present address. Stanford Cancer Center, Stanford, CA, USA.
†† Present address. CHRISTUS Good Shepherd/Texas A&M University Internal Medicine Residency Program, Longview, TX, USA.
‡‡ Present address. School of Medicine and Dentistry, University of Rochester, Rochester, NY, USA.
¶¶ Present address. Division of Cardiovascular Health and Disease, University of Cincinnati, Cincinnati, OH, USA.

Graphical Abstract

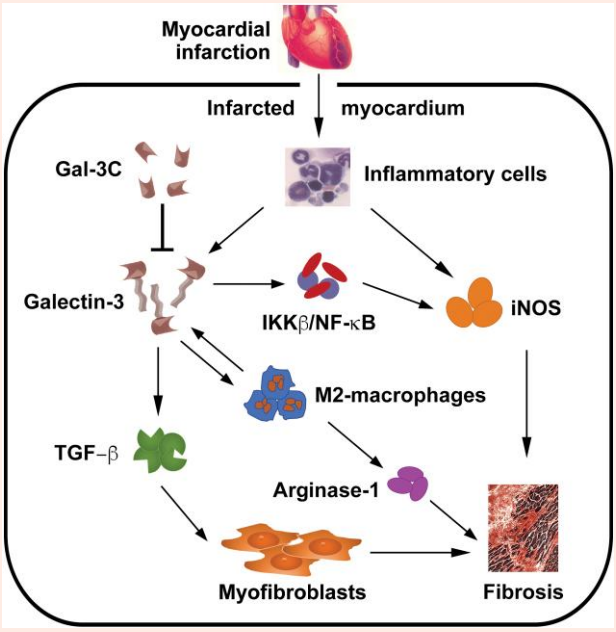

Galectin-3-mediated pathways driving fibrosis in the infarcted myocardium. MI triggers the increased secretion of galectin-3 by inflammatory cells that contribute to myofibroblast activation via the TGF-β pathway, the increased expression of arginase-1 via the M2-macrophage alternative pathway that activates a galectin-3 positive feedback loop, and the galectin-3 mediated up-regulation of iNOS via the IKKβ/NF-κB pathway. The inhibition of galectin-3 by Gal-3C regulates these post-MI inflammatory profibrotic signalling cascades, resulting in therapeutic benefits in acute MI models of young and aged hearts.

Keywords Galectin-3 • Heart failure • Inducible nitric oxide synthase • Fibrosis • Myocardial infarction

1. Introduction

Heart failure (HF) is an end-stage of many heart diseases including and most commonly myocardial infarction (MI). Acute MI causes an immediate and robust inflammatory response that leads to increased myocardial collagen deposition and reparative fibrosis secondary to cardiomyocyte death.[1] While regional inflammation and fibrosis promote healing of the infarcted myocardium, adverse remodelling of viable myocardium begins as well. This remodelling involves a pathological myocardial fibrotic process commonly referred to as reactive fibrosis, which is characterized by excessive fibrosis and ultimately accelerates the progression to HF. Thus, myocardial fibrosis is a major contributor to the adverse remodelling that is a key mechanism of HF. However, how or when to limit excessive fibrosis to achieve optimal therapeutic outcomes remains unclear.[2] Likewise, much remains to be learned about the potential involvement of negative regulatory mechanisms that confine profibrotic signals, in the restriction of uncontrolled fibrosis following MI.

Post-MI myocardial fibrosis, which encompasses both replacement fibrosis and reactive interstitial fibrosis, is caused by fibroblast differentiation and excessive extracellular matrix (ECM) deposition. Interstitial fibrosis is a result of the influence of MI-induced inflammation on ECM remodelling, which provides structural integrity to the dying region of the myocardial wall, but reduces ventricular compliance associated with the development of subsequent HF. Unchecked fibrosis in the periinfarct zone interferes with both systolic and diastolic function after MI. Thus, reducing cardiac fibrosis at the appropriate time during post-MI remodelling is expected to attenuate long-term ventricular dysfunction so as to minimize the development of HF after MI and improve patient outcomes. There is an unmet medical need for new therapeutic agents, particularly those with novel mechanisms of action, despite the existence of drugs that are currently available to treat post-MI HF, such as angiotensin II receptor blockers (ARBs) and mineralocorticoid receptor antagonists (MRAs), which exert modest antifibrotic effects as secondary modes of action.[3,4]

Galectin-3 is a β-galactoside-binding lectin that has been implicated as a major mediator of inflammation and organ fibrosis.[5–8] Galectin-3 crosslinks the glycoprotein receptors for growth factors such as transforming growth factor (TGF)-β and vascular endothelial growth factor (VEGF), thereby preventing the endocytosis of their receptors and facilitating growth factor signalling.[9] In the heart, up-regulation of galectin-3 induces cardiac fibroblasts to proliferate and differentiate into myofibroblasts, thereby enhancing collagen deposition, increasing interstitial fibrosis, and pathological remodelling.[8] Importantly, an elevated plasma level of galectin-3 is correlated with adverse outcomes in both HF with reduced and preserved ejection fraction (HFrEF and HFpEF) phenotypes,[10,11] and has been approved in the USA and the European Union as a prognostic risk indicator for HF.[12]

We have developed a dominant negative inhibitor of galectin-3 (Gal-3C, MM-003) based on its C-terminal carbohydrate recognition domain (CRD).[13] Since post-MI HFrEF is characterized by cardiomyocyte loss, and reparative fibrosis reduces ventricular elasticity and distensibility, causing diastolic dysfunction that exacerbates HF, we hypothesized that the treatment of the infarcted heart with Gal-3C to limit interstitial fibrosis would attenuate fibrotic remodelling and cardiac dysfunction. Our findings show that 7-day administration of Gal-3C limited excessive fibrosis by impeding galectin-3-mediated profibrotic effects of inducible nitric oxide synthase (iNOS) and alternative M2-macrophage-mediated-arginase-1 to substantially restrict ventricular enlargement and attenuate diastolic dysfunction over 56 days post-MI. These effects were apparent in multiple models of MI in young and aged rats and were significantly better than those of the ARB, losartan, and the MRA, spironolactone. The antifibrotic efficacy of Gal-3C provides a new therapeutic opportunity for MI patients with developing HFrEF.

2. Methods

All procedures involving animals were approved by the Institutional Animal Care and Use Committee of the University of California, San Francisco (UCSF), USA. All experiments were performed according to the UCSF guidelines for rodent survival surgery and the Guide for the Care and Use of Laboratory Animals of the National Institutes of Health (USA).

2.1 Rats and mice

Male Sprague–Dawley rats at age 10–12 weeks were randomly assigned to the experimental groups. Rats were housed in a temperature-controlled room with 12 h light/12 h dark cycle and given regular chow. Typical experimental group size was $n = 10$ (see Statistics). Rats were purchased from Simonsen Laboratories (Santa Clara, CA, USA) and Charles River Laboratories (Wilmington, MA, USA). A disease outbreak in the Simonsen colony required us to change vendors during the project. For experiments with aged animals, male Fischer 344 rats at 1.5 years of age were obtained from the National Institute on Aging, USA. Three Fischer 344 rats were excluded due to jaundice in the skin. Male C57BL/6J mice at age 10 weeks were purchased from the Jackson Laboratory (Bar Harbor, ME, USA).

2.2 Production and analyses of Gal-3C

Human Gal-3C, a 143 amino acid protein, was produced by two methods. Initially, Gal-3C was produced by enzymatic cleavage of full-length galectin-3, denoted as Gal-$3C_{CL}$. Subsequently, Gal-3C was directly expressed in final form in *Escherichia coli* (Gal-$3C_{EXP}$), because this method would be more amenable to industrial-scale production. Detailed methods for production and analyses of Gal-3C are provided in the Supplementary material online, *Methods*.

2.3 Gal-3C delivered intravenously from osmotic pumps

ALZET osmotic pumps were implanted subcutaneously immediately before surgical induction of MI ('early window') or 4 days post-MI ('delayed window') to deliver Gal-3C and vehicle (phosphate-buffered saline with lactose; Supplementary material online, *Methods*) over 7 days.

2.4 Hydroxyproline assay for collagen in the heart

Rats were euthanized and the left ventricular (LV) tissue was homogenized for the analysis of hydroxyproline, an amino acid found in collagen (see Supplementary material online, *Methods*).

2.5 Galectin-3 measurement in mice

Serum levels of galectin-3 in healthy and MI mice were analysed by ELISA (see Supplementary material online, *Methods*).

2.6 Losartan and spironolactone treatments

Losartan was administered starting the same day of the MI and continuously over the 56-day experiment. Spironolactone was administered starting at 4 days post-MI and continuing for the first 28 days of the 56-day experiment (see Supplementary material online, *Methods*).

2.7 Myocardial infarction

Surgical MI was induced in rats and mice receiving anaesthesia with 2% isoflurane and analgesics (buprenorphine at 0.1 mg/kg, subcutaneous injection pre- and post-operation and afterward once per day over 3 days) (see Supplementary material online, *Methods*). MI surgical procedure involved either an ischaemia–reperfusion (I/R) with a temporary occlusion (25 min) of the left anterior descending coronary artery (LAD) or permanent LAD ligation. For euthanasia, rats and mice were anaesthetized with 5% isoflurane for 5 min, and the heart was removed after confirmation that there was a lack of active paw reflex.

2.8 Echocardiography

Serial echocardiography was performed at baseline, and 2, 28, or 56 days post-MI. Investigators who measured echocardiographic parameters were blinded to group identity (see Supplementary material online, *Methods*).

2.9 Haemodynamic data acquisition and analysis

Intraventricular haemodynamic variables were continuously recorded on Day 28 or 56 post-MI (see Supplementary material online, *Methods*).

2.10 Measurement of infarct scar size

Heart cryosections were stained with Masson's trichrome for infarct scar size measurement (see Supplementary material online, *Methods*). Sections were analysed by blinded investigators.

2.11 Quantitative analysis of non-scar fibrosis

One cryosection/heart was stained with Sirius red for quantitative analysis of fibrotic collagen (red). Non-scar fibrosis was measured by a blinded investigator using two different approaches (see Supplementary material online, *Methods*).

2.12 Inhibition of the activation of M2-polarized human monocytes

Protocol for M2-polarized human monocyte activation by exposure to interleukin (IL)-4 and subsequent inhibition by Gal-3C treatment with measurements of arginase-1 and IL-10 released by polarized monocytes can be found in the Supplementary material online, *Methods*.

2.13 ELISA for arginase-1, IL-10, and IL-6

Rat plasma samples were obtained for measurements of arginase-1, IL-10, and IL-6 by ELISA (see Supplementary material online, *Methods*).

2.14 Immunoblot analyses for arginase-1, iNOS, inhibitor of NF-κB kinase (IKK), NF-κB P65, and protein kinase B (Akt)

The LV tissue was harvested and homogenized for analyses of immunoblots (see Supplementary material online, *Methods*).

2.15 Sorting M1 and M2 macrophages from infarcted hearts by flow cytometry

For macrophage detection, cell suspensions of digested LV tissues were incubated with antibodies for CD45 (leucocyte common antigen), CD86 (M1 marker), and CD163 (M2 marker) for membrane detection, and CD68 (PAN macrophage marker) for intracellular staining. M1 and M2 macrophages were identified as $CD45^+CD68^+CD86^+$ and $CD45^+CD68^+CD163^+$ by flow cytometry (see Supplementary material online, *Methods*).

2.16 Statistics

A power calculation based on standard deviations from within-group comparisons in several of our previous MI experiments determined that $n = 10$/group was sufficient to detect changes in cardiac function at a power of 0.8 and a significance level of 0.05. For comparisons involving multiple groups and times, we fit a 2-factor (treatment condition and time) repeated-measures analysis of variance to all the data at once using a mixed model estimated with restricted maximum likelihood estimation with an unstructured covariance matrix of residuals, then tested for differences over time

and across treatment condition using contrasts and pairwise comparisons, adjusted for multiple comparisons using the Šidák method. Comparisons of multiple groups at one time point (terminal) were analysed using one-way analysis of variance followed by the Šidák multiple comparison test. Calculations were done with Stata 13.1. Simple comparisons of two groups with control and treatment were analysed using Student's unpaired *t*-test. All data are means ± standard deviations (SD).

3. Results

3.1 Short-term Gal-3C treatment beginning at 4 days post-MI was efficacious in an I/R model of MI

Therapy that begins before an MI is of limited clinical relevance. We reasoned that a delayed treatment might limit the long-term pathological fibrotic response while still allowing the earlier fibrotic repair of the infarct. Therefore, a 'delayed window' experiment was carried out with Gal-3C continuous delivery from implanted osmotic pumps starting at 4 days post-MI over 7 days. The Gal-3C was produced by enzymatic cleavage of full-length galectin-3, Gal-3C$_{CL}$ (see Supplementary material online, *Methods*). The period chosen for delayed administration was based on the timing of the peak levels of galectin-3 in mice (see Supplementary material online, *Figure S1A*) and rats post-MI,[14] and on a pilot experiment to determine collagen levels in post-MI hearts treated with Gal-3C (see Supplementary material online, *Results* and *Figure S1B*). Animals receiving Gal-3C obtained significant benefits in 28-day EF and end-systolic volume (ESV) as measured echocardiographically (*Figure 1A* and Supplementary material online, *Table S1*), but not end-diastolic volume (EDV). Haemodynamic parameters indicated functional improvement with significantly increased LV end-systolic pressure (ESP), decreased end-diastolic pressure (EDP), and improved dP/dt_{max} and dP/dt_{min} in the Gal-3C group (*Figure 1B* and Supplementary material online, *Table S3*; all haemodynamic parameters are defined in Supplementary material online, *Table S2*). Gal-3C therapy limited the infarct scar size (*Figure 1C*) and also inhibited non-scar fibrosis measured by two different approaches (explained in Supplementary material online, *Figure S3*) each by ~65% compared with vehicle controls (*Figure 1D*).

A similar experiment in which Gal-3C 7-day delivery began shortly before the MI ('early window') resulted in similar therapeutic effects (see Supplementary material online, *Results*, *Figure S4*, and *Tables S4 and S5*).

3.2 Gal-3C treatment was superior to losartan for therapy of I/R MI

ARBs such as losartan are recommended as one of the classes of agents used in HF. Angiotensin II, which is formed from angiotensin I by angiotensin-converting enzyme (ACE), is a vasoconstrictor that also stimulates aldosterone secretion and induces the expression of TGF-β and cardiac fibrosis by macrophages and myofibroblasts post-MI.[15] We therefore compared the therapeutic effect of Gal-3C post-MI with that of losartan at its optimal dosage regimen,[4] using the Gal-3C$_{CL}$ form. For this experiment, we waited until 56 days post-MI for our final measurements because the previous experiments had revealed no difference in EDV between vehicle and Gal-3C groups at 28 days (*Figure 1A*), presumably because more diastolic dysfunction occurred at a later time point in the remodelling process. Losartan was administered starting later the same day of the MI and continuously over the 56-day experiment at 8 mg/kg/day in the drinking water. As before, 28-day post-MI, Gal-3C significantly improved EF and ESV but not EDV; however, by 56 days post-MI, improvement was observed in EDV (*Figure 2A* and Supplementary material online, *Table S6*). In contrast, there was a lesser benefit from losartan relative to vehicle 28-day post-MI; EF stayed lower in this group and there were increased ESV and EDV at 56 compared with 28 days post-MI in both losartan and vehicle groups. Haemodynamic parameters, including ESP, EDP, dP/dt_{max}, dP/dt_{min}, and Tau, were significantly improved by Gal-3C (*Figure 2B* and Supplementary material online, *Table S7*), evidencing functional improvements at systole and diastole. Furthermore, Gal-3C was more effective than losartan in limiting infarct size and interstitial fibrosis (significance for infarct size defined as $P < 0.05$ was barely missed; $P = 0.053$ and 0.062 vs. vehicle and losartan, respectively) (*Figure 2C* and *D*).

3.3 Gal-3C produced by enzymatic cleavage of full-length galectin-3 or by direct expression of the truncated form led to comparable therapeutic efficacy in I/R MI

Gal-3C consists of the carboxy-terminal residues of human galectin-3 containing the CRD. Gal-3C uniquely inhibits galectin-3 by dual mechanisms. It binds to the galectin-3 CRD and to carbohydrates that are ligands for galectin-3. To increase translatability, we assessed the therapeutic efficacy of Gal-3C produced by enzymatic cleavage of galectin-3 (Gal-3C$_{CL}$) to that of Gal-3C directly expressed in *E. coli* not requiring any enzymatic digestion (Gal-3C$_{EXP}$) (see Supplementary material online, *Methods*). We reasoned that Gal-3C$_{EXP}$ would be more clinically translatable than Gal-3C$_{CL}$, because Gal-3C$_{EXP}$ was made using a process more amenable for scaled-up production. We compared responses at 28 and 56 days to Gal-3C$_{EXP}$ and Gal-3C$_{CL}$ at the dose of 600 µg/day with intravenous administrations beginning at 4 days post-MI (delayed window). As expected, the post-MI cardiac function was better with Gal-3C$_{EXP}$ therapy including more improved EF on Days 28 and 56 and smaller ESV on Day 28 compared with Gal-3C$_{CL}$ therapy at the same dose and timing (see Supplementary material online, *Figure S5A* and *Table S8*). Haemodynamics on Day 56 indicated significantly better EF, CO, and Ea from Gal-3C$_{EXP}$ therapy, although Gal-3C$_{CL}$ therapy led to smaller EDV (see Supplementary material online, *Figure S5B* and *Table S9*). The result indicates that Gal-3C$_{EXP}$ was more or equally therapeutically efficacious.

3.4 Short-term Gal-3C treatment had dose-responsive efficacy for I/R MI therapy

To determine the optimal dosage of Gal-3C$_{EXP}$ for our subsequent rat experiments, we performed a dose–response experiment, comparing the delivery of vehicle with that of Gal-3C$_{EXP}$ at 100, 600, or 1500 µg/day (~0.4, 2.4, and 6 mg/kg) for 7 days beginning at 4 days post-MI (delayed window).

EF on Days 28 and 56 of rats treated with 600 µg/day of Gal-3C was significantly improved compared with rats receiving either of the other two doses, and ESV on Day 56 of rats treated with 600 µg/day was significantly smaller compared with 100 µg/day (*Figure 3A* and Supplementary material online, *Table S10*). Importantly, Gal-3C at 600 µg/day substantially lowered EDV at both 28 and 56 days. Also, Gal-3C at 600 µg/day led to better haemodynamics based on EF and cardiac output (CO), and reduced arterial stiffness (arterial elastance, Ea) compared with 100 or 1500 µg/day (*Figure 3B* and Supplementary material online, *Table S11*). However, a dose of 100 µg/day led to better ESP ($P < 0.05$) and a trend towards a better mean arterial pressure (MAP; $P = 0.057$) and dP/dt_{max} ($P = 0.074$) compared with 1500 µg/day.

Overall, comparing both echocardiographic and haemodynamic measurements, the therapeutic effects were best in rats treated with 600 µg/day compared with either 100 or 1500 µg/day. Thus, the 600 µg/day dose indicated a peak in efficacy that was reduced at the higher or lower doses, although echocardiographic results showed that all three dosage levels improved diastolic function by reduction of EDV. Based on these results, 600 µg/day was used for all subsequent experiments. These results indicate that Gal-3C improves not only systolic function but also diastolic function, evident if outcomes are determined at 56 days post-MI.

3.5 Efficacy of Gal-3C monotherapy was superior to spironolactone or losartan, and was not additionally improved by co-treatment with losartan for I/R MI

Spironolactone is thought to act via the mineralocorticoid receptor to reduce cardiac fibrosis after MI by blocking the action of aldosterone.[4] Although there is no evidence that galectin-3 has direct glucocorticoid

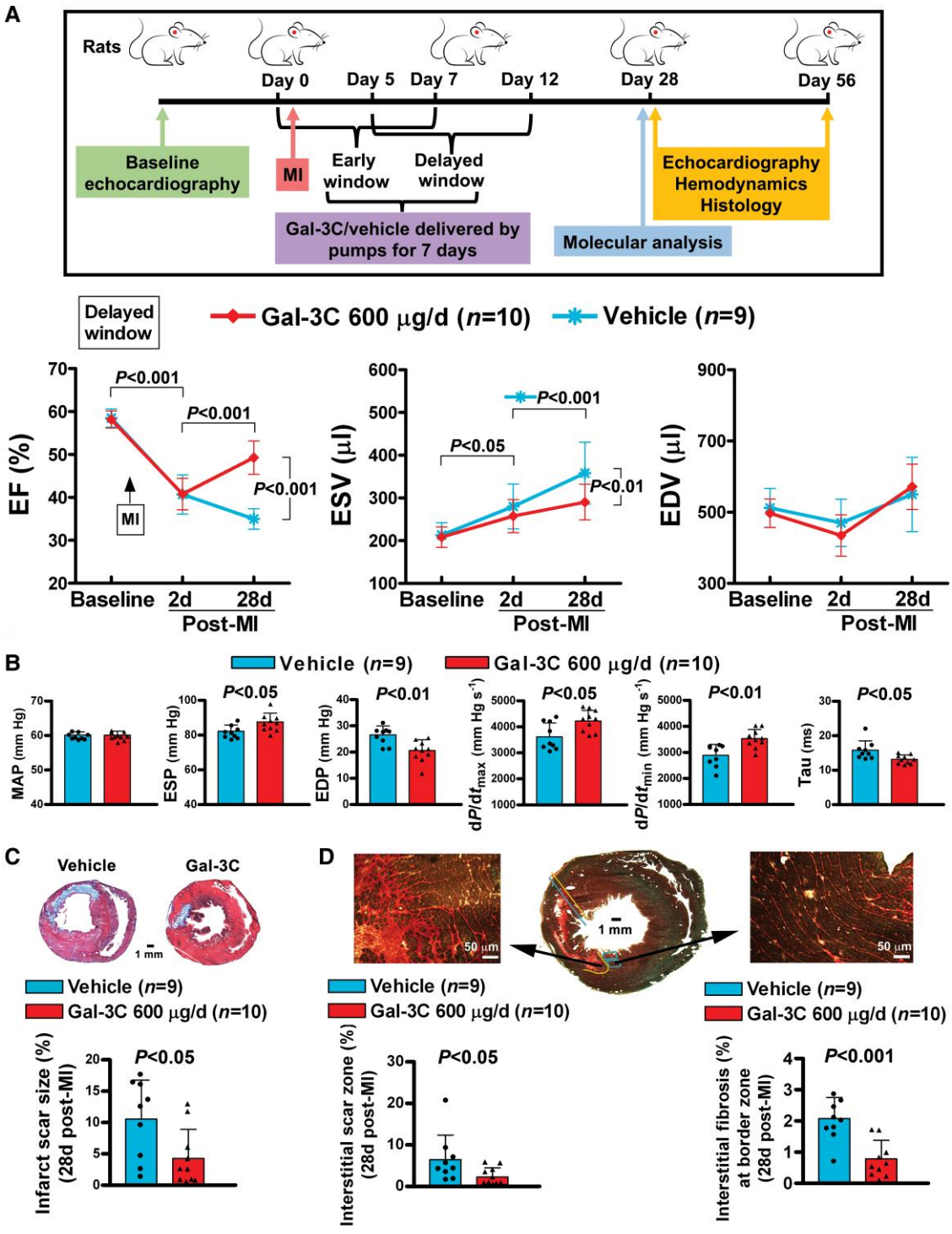

Figure 1 Therapeutic effect of Gal-3C delayed-window administration on cardiac function and fibrosis after I/R MI. (*A*) Workflow and cardiac function by echocardiography. (*B*) Haemodynamic parameters 28-day post-MI. (*C*) Infarct scar size. Representative single section from each of the two groups shows the maximum infarct size in each heart with the median infarct size values for each group. Eight to 10 cryosections from the apex to base of the ventricle were stained with Masson's trichrome for infarct scar size measurement (see Supplementary material online, *Figure S2*). (*D*) Interstitial (non-scar) fibrosis. One cryosection containing the most scar from each heart as determined by the trichrome results was stained with Picro-Sirius red for the quantitative analysis of non-scar fibrosis. Interstitial fibrosis was measured by two different approaches at the interstitial scar zone and infarct border zone. The interstitial scar zone is the area of the tissue containing thick bundles of fibrosis around the scar; interstitial fibrosis is the per cent of tissue containing fibrosis-stained pixels at the infarct border zone (see Supplementary material online, *Figure S3*). Abbreviations are as in Supplementary material online, *Tables S1* and *S2*. Number in (*A*–*D*): vehicle, $n = 9$; Gal-3C, $n = 10$. Statistical tests: two-way ANOVA followed by the Šidák method (*A*); Student's unpaired *t*-test (*B*–*D*).

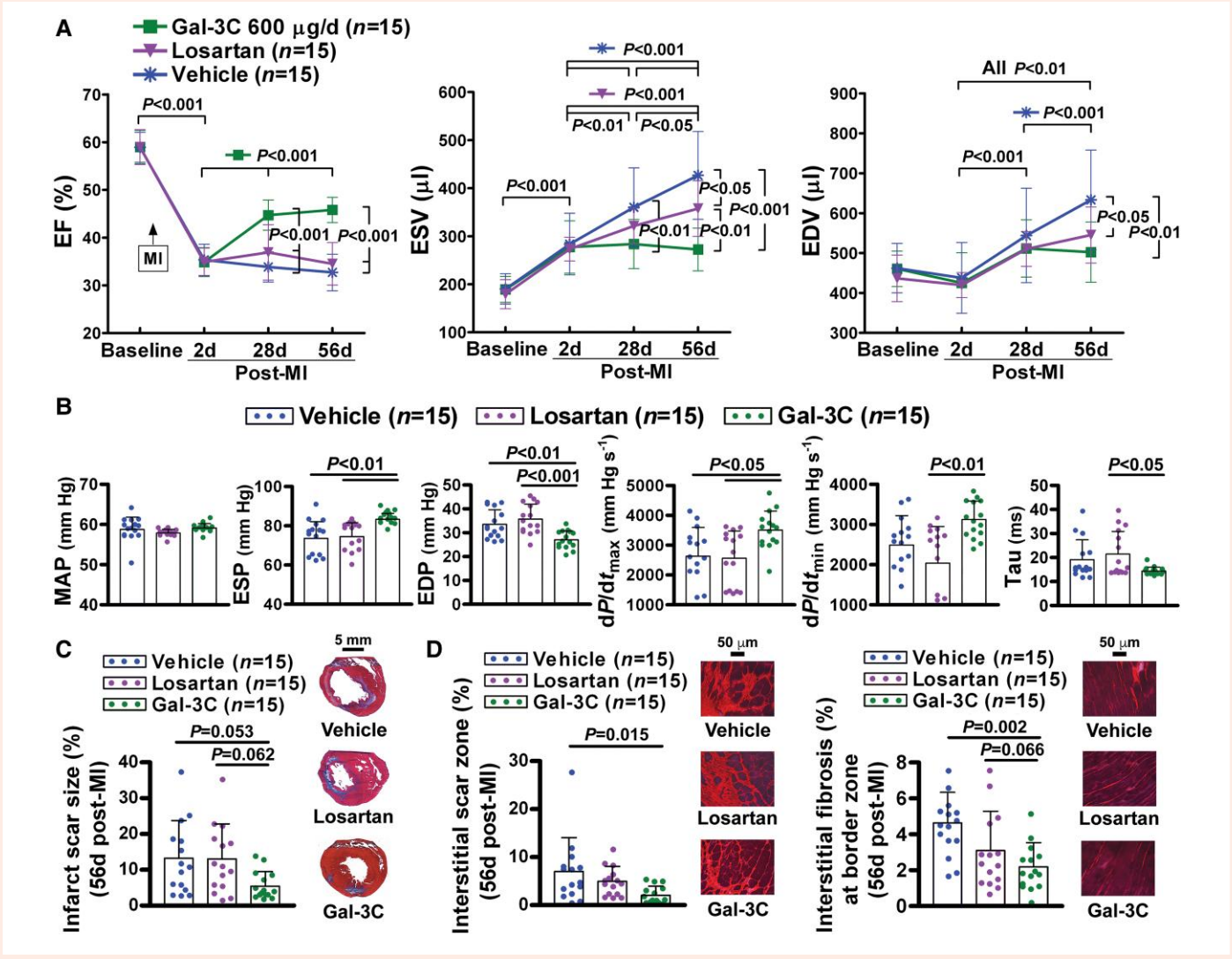

Figure 2 Therapeutic effect of Gal-3C compared with the losartan therapy in the delayed-window post-I/R MI. (*A*) Comparison of cardiac function in Gal-3C$_{CL}$ vs. losartan-treated groups post-MI. (*B*) Haemodynamics of the artery and intraventricular pressures measured on Day 56 post-MI. (*C*) Infarct scar size. (*D*) Interstitial fibrosis. Number in (*A–D*): $n = 15$ each group. Statistical tests: two-way (*A*) and one-way (*B–D*) ANOVA followed by the Šidák method.

activity, expression of galectin-3 is up-regulated by aldosterone; and profibrotic effects of aldosterone were shown to be inhibited by a galectin-3 inhibitor, modified citrus pectin.[7] Therefore, we postulated that Gal-3C could act downstream of aldosterone to inhibit fibrosis. Having already compared Gal-3C with losartan therapy (*Figure 2A–D*), we now compared the benefits of Gal-3C with spironolactone, and compared Gal-3C or losartan alone with losartan/Gal-3C combination therapy to determine if the effects of losartan are further improved by combination with Gal-3C, given their different mechanisms of actions.

The animals were randomized into five groups receiving the following five treatment conditions as depicted in *Figure 4A*: Gal-3C, spironolactone, losartan, Gal-3C and losartan together, and vehicle. The Gal-3C$_{EXP}$ form was delivered beginning at 4 days post-MI (delayed window), using the best therapeutic dosage (600 μg/day) from the dose–response experiment, and the vehicle received PBS/lactose from pumps using the same timing. Detailed administrations of spironolactone[4] and losartan are described in the Supplementary material online, *Methods*. Rats treated with spironolactone or losartan alone had an appreciable benefit in EF 28 and 56 days post-MI, relative to vehicle controls, but the improvement in EF was significantly less than that of Gal-3C alone or of combination with losartan (*Figure 4A* and Supplementary material online, *Table S12*). Gal-3C alone and with losartan also limited the increase in 28-day ESV, and conserved ESV and EDV from Days 28 to 56. However, combination therapy was no more efficacious than Gal-3C alone, likely because most of the benefits of losartan on cardiac remodelling are mediated by downstream effects on galectin-3. Consistent with the results from echocardiography, haemodynamics demonstrated benefits in EF, ESV, EDV, and CO from both Gal-3C alone and combination therapy, which, in conjunction with the 56-day benefit in EDV, indicates a diastolic functional benefit (*Figure 4B* and Supplementary material online, *Table S13*). These findings strongly indicate that Gal-3C treatment of cardiac remodelling post-MI and in some forms of HF could be more effective than standard MRA/ARB therapies.

3.6 Short-term treatment with Gal-3C was highly efficacious in an aged rat model of I/R MI

All experiments described above were done with young rats. However, MI typically manifests in individuals who are middle-aged and older, ages at

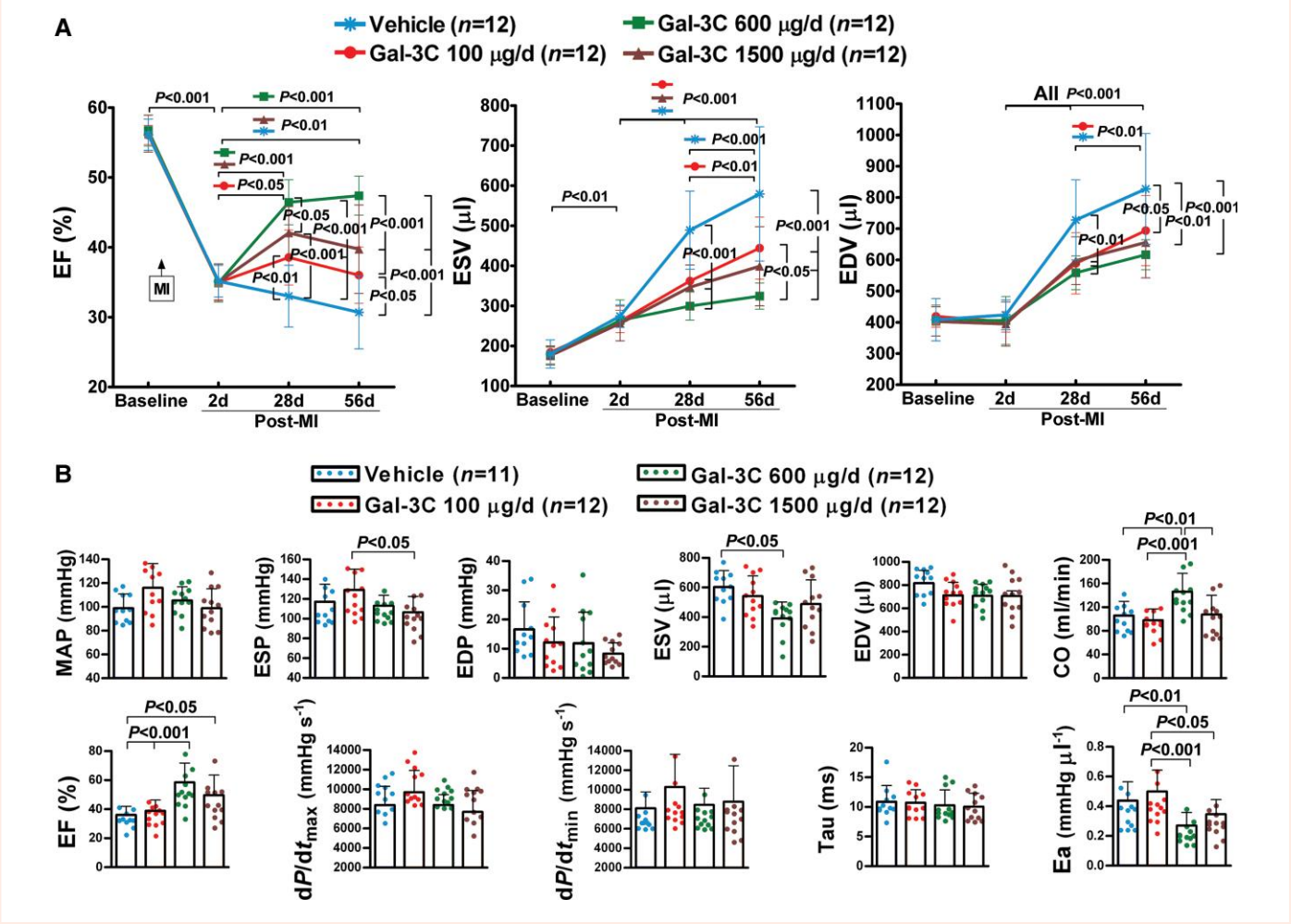

Figure 3 Echocardiographic and haemodynamic functional changes in Gal-3C dose–response experiments. (*A*) Echocardiographic parameters. (*B*) Haemodynamics using pressure–volume (PV) loops. Number in (*A* and *B*): $n = 12$ each group. Statistical tests: two-way (*A*) and one-way (*B*) ANOVA followed by the Šidák method.

which cardiac fibrosis is more prevalent in otherwise healthy individuals.[16] Even in the absence of MI, the ageing heart undergoes fibrotic remodelling, characterized by accumulation of interstitial collagen, leading to diastolic dysfunction and HF. Thus, age-associated cardiac fibrosis might exacerbate adverse post-MI dilative remodelling and create an environment less amenable to the antifibrotic effects of Gal-3C. To more realistically reflect a typical clinical scenario, we administered 600 μg/day of Gal-$3C_{EXP}$ to 1.5-year-old Fischer 344 rats (which were available to us from the National Institute on Aging's Aged Rodent Colony), using the delayed-window timing of 7 days starting at 4 days post-MI. We included a vehicle group and a sham-surgery group (opening the chest and passing a suture through the myocardium without tying off the coronary artery but still receiving a vehicle pump). Echocardiography revealed that the aged rats treated post-MI with Gal-3C dramatically benefited with improved EF 28-day post-MI and continued improvement of EF and complete prevention of increase in ESV by 28 and 56 days (*Figure 5A* and Supplementary material online, *Table S14*). Impressively, EF in Gal-3C-treated rats was fully restored to the level of sham-operated rats. Haemodynamics indicated powerful functional improvements in EF, CO and stroke work (SW), reduced ESV, and decreased Ea in post-MI ageing rats treated with Gal-3C vs. vehicle (*Figure 5B* and Supplementary material online, *Table S15*). There was a trend but not a statistically significant benefit in EDV in the echocardiographic and haemodynamic analyses. These results demonstrate that in aged rats, treatment with Gal-3C post-MI substantially improves pump function and restricts ventricular dilation at systole, thus preventing adverse dilative remodelling and HF post-MI.

3.7 Gal-3C treatment was efficacious in a permanent ligation model of MI

While I/R MI reflects the tissue milieu in post-MI patients who have undergone catheterization to open the blocked artery, more extreme tissue remodelling occurs after a permanent occlusion, mimicked in rodents as a coronary artery permanent ligation MI model. Because permanent ligation leads to more pronounced ventricular wall thinning at the scar, we determined whether Gal-3C therapy would be beneficial in this model. As was the case for I/R MI, Gal-3C treatment for permanent ligation MI (using delayed-window timing of 7 days starting at 4 days post-MI) led to a striking benefit in echocardiographic parameters, improving EF while preventing an increase in ESV and EDV by 28 and 56 days post-MI (see Supplementary material online, *Figure S6* and *Table S16*). There were significant differences in haemodynamic ESP and dP/dt_{min} between Gal-3C and vehicle groups (see Supplementary material online, *Table S17*). Notably, Gal-3C therapy for permanent ligation MI provided a clear benefit in EDV by 28 days post-MI, whereas benefit in the I/R MI model was not observed until the 56-day time point (*Figure 2A*).

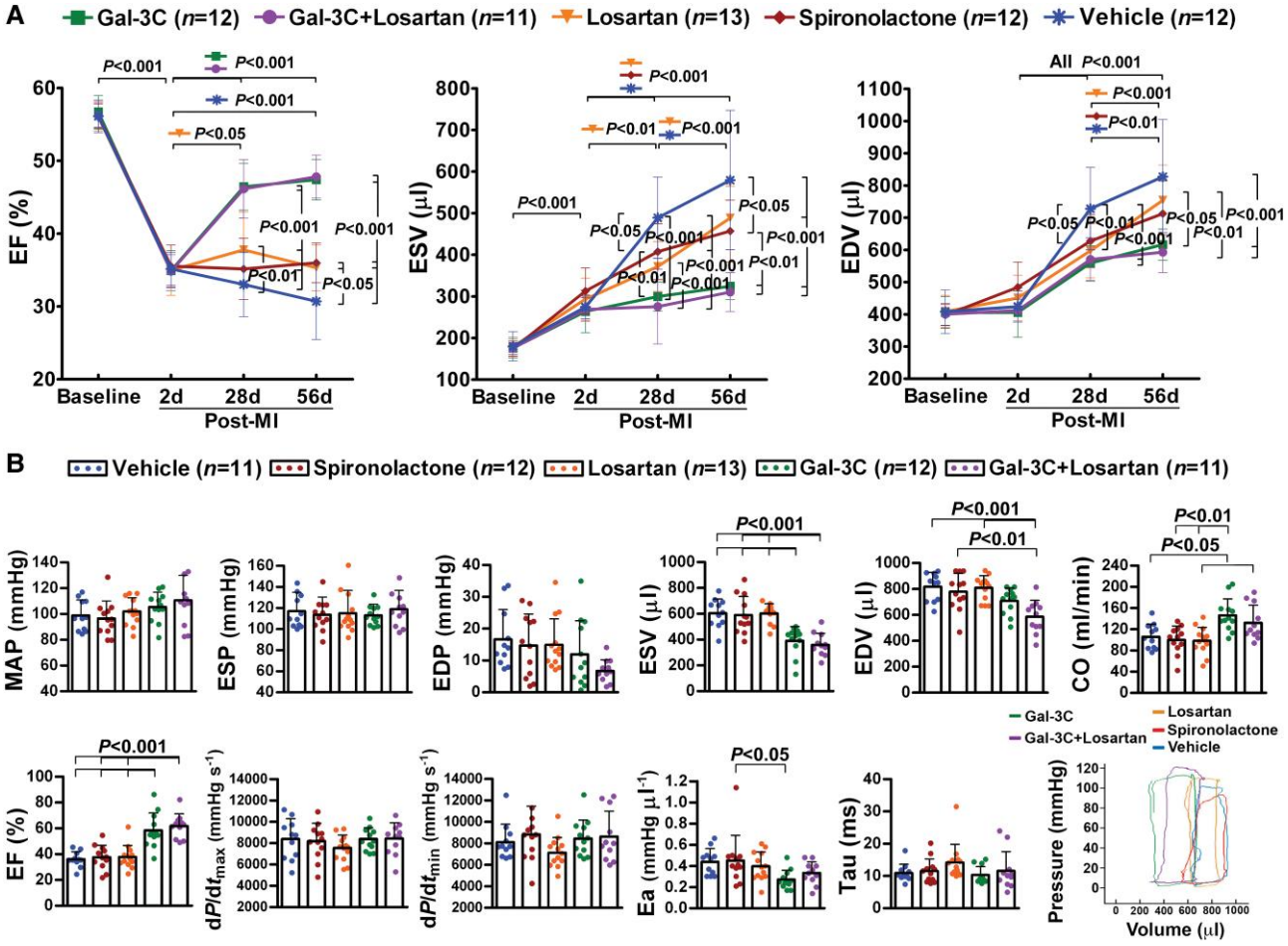

Figure 4 Analysis of therapeutic effects of Gal-3C compared with two current cardiovascular drugs and in combination therapy post-MI. (*A*) Comparison of echocardiographically measured cardiac function in Gal-3C$_{EXP}$, losartan, and spironolactone vs. the combination of Gal-3C$_{EXP}$ with losartan-treated groups. (*B*) Haemodynamics quantified on Day 56 post-MI. Number in (*A* and *B*): $n = 11–13$ each group. Statistical tests: two-way (*A*) and one-way (*B*) ANOVA followed by the Šidák method.

3.8 Gal-3C inhibited the M2 polarization of human macrophage-like cells *in vitro* and reduced their phenotypic expression of arginase-1 and IL-10

During injury-healing, macrophages acquire an anti-inflammatory profibrotic M2 phenotype, induced by M2-cytokines IL-4 and IL-13. These 'alternatively activated' macrophages express the mannose receptor (CD206) and secrete profibrotic and anti-inflammatory cytokines such as IL-10 and TGF-β that promote cardiac tissue repair. Galectin-3 is secreted by M2 macrophages and, furthermore, induces continued M2 polarization of macrophages via a positive feedback loop that results in the sustained activation of PI3K.[5] Therefore, we tested whether Gal-3C exposure could limit the differentiation to the M2-phenotype in a model of human macrophages by measuring levels of two M2-markers, arginase-1 and IL-10.[5] We treated human monocytic THP-1 cells with phorbol-12-myristate-13-acetate (PMA) to induce differentiation into macrophage-like cells *in vitro*, exposed them to IL-4 to polarize them into an M2 phenotype, and measured arginase-1 and IL-10 in the absence and presence of Gal-3C$_{EXP}$. Exposure to IL-4 substantially increased the expression of arginase-1 and IL-10, but this expression was significantly reduced in the presence of Gal-3C (*Figure 6A*). These results provide evidence that Gal-3C can reduce the polarization of macrophages to the M2 wound-healing phenotype, therefore limiting fibrosis induced by organ injury.

3.9 Gal-3C treatment post-MI down-regulated myocardial iNOS expression through signalling of IKKβ/NF-κB along with alternative reductions in arginase-1 expression

While the *in vitro* modulation of macrophage polarization by Gal-3C shown in *Figure 6A* is consistent with Gal-3C's antifibrotic effects *in vivo*, we also examined the *in vivo* effects of Gal-3C on profibrotic signalling pathways with a focus on arginase-1 and iNOS, both co-expressed by macrophages in which polarization along the M1 (classical) or M2 (alternative) axis occurs depending on the inflammatory circumstance.[17] In MI patients, plasma levels of arginase-1 are continuously elevated and involved in the development of MI.[18] In the failing heart, iNOS is derived from both infiltrating leucocytes and cardiomyocytes. Importantly, leucocyte-localized up-regulated iNOS accelerates remodelling and HF progression post-MI.[19,20] IKK and its downstream target NF-κB, which regulates iNOS expression, are master regulators of inflammation, implicated in

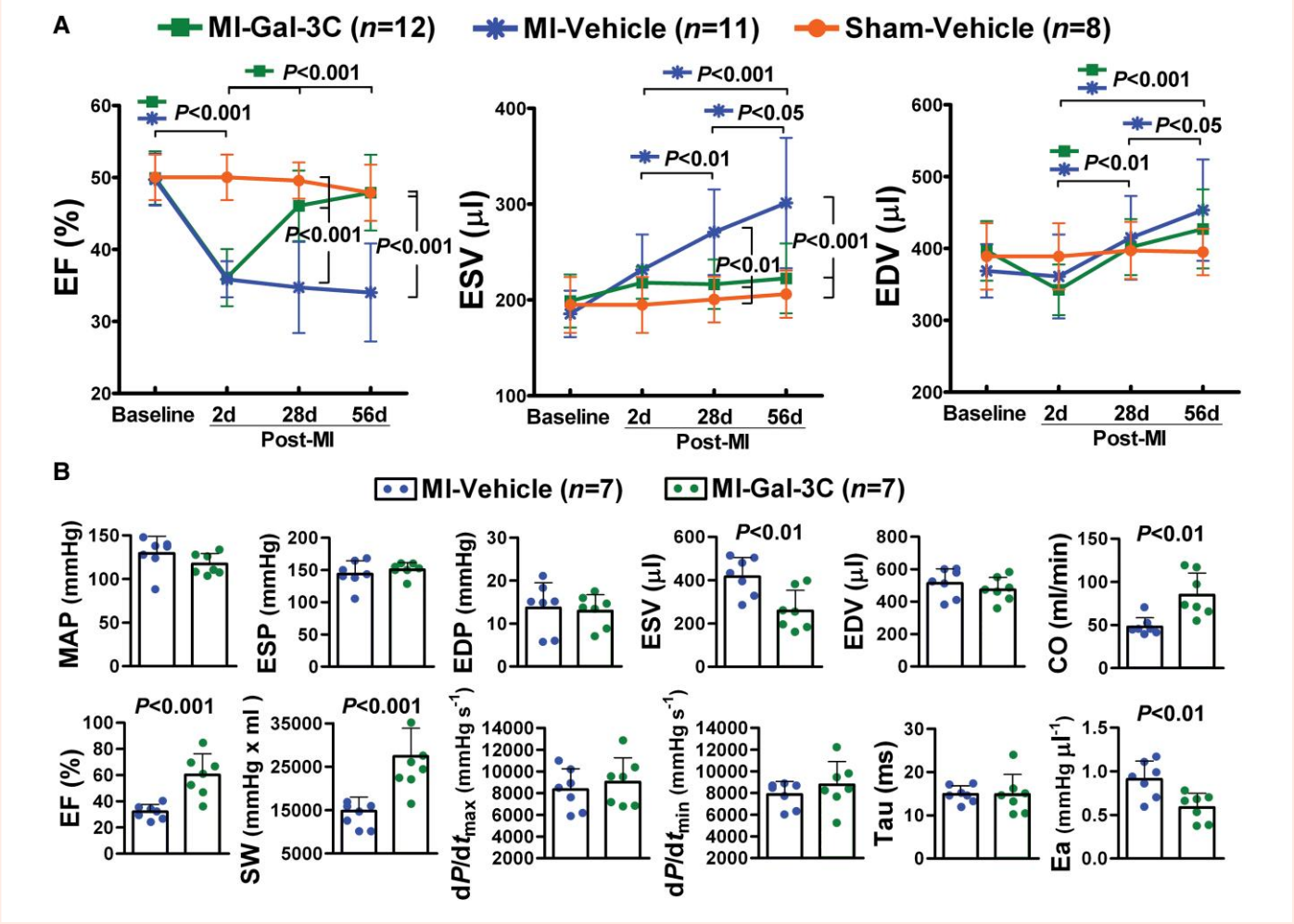

Figure 5 Functional improvements by 7-day treatment with Gal-3C after I/R MI in aged Fischer rats. (*A*) Cardiac function from serial echocardiography. (*B*) Haemodynamic changes at systole and diastole. Number in (*A*): MI-Gal-3C, $n = 12$; MI-Vehicle, $n = 11$; Sham-Vehicle, $n = 8$. Number in (*B*): $n = 7$ each group. Statistical tests: two-way ANOVA followed by the Šidák method (*A*); Student's unpaired *t*-test (*B*).

inflammatory dilated cardiomyopathy, I/R damage, MI, and HF.[1,21] Protein kinase B (Akt) is also an important modulator of proinflammatory signal-dependent expression of iNOS. Notably, Gal-3C inhibited the Akt/IKK/NF-κB pathway in ovarian and multiple myeloma cell lines.[22] However, galectin-3-mediated arginase-1 in conjunction with altered iNOS in promoting post-MI cardiac fibrosis progression is poorly understood. Therefore, in accordance with the *in vitro* down-regulated arginase-1 expression by Gal-3C in *Figure 6A*, we investigated whether Gal-3C *in vivo* therapy would restrain myocardial arginase-1 and iNOS expression to ultimately impede fibrosis post-MI through signalling of IKK/NF-κB or Akt.

Given that peak levels of galectin-3 occurred within 7 days post-MI in mice (see Supplementary material online, *Figure S1A*) and in rats,[14] along with increased leucocyte infiltration into the infarct,[23] and that 7-day administration of Gal-3C led to significant functional improvement by Day 28 post-MI, we measured post-MI plasma levels of arginase-1, IL-10, and IL-6, and analysed levels of arginase-1, iNOS, IKK, NF-κB P65, and Akt in the LV tissue 28-day post-MI. Gal-3C early therapy significantly reduced plasma levels of arginase-1 (*Figure 6B*) and IL-6 (see Supplementary material online, *Figure S7*) on Day 28 post-MI, whereas the delayed treatment did not change levels of arginase-1 and neither early nor delayed treatment changed levels of IL-10 (*Figure 6B*). Notably, Gal-3C delayed-treatment down-regulated myocardial iNOS expression ($P = 0.049$) compared with vehicle, with reductions in arginase-1 expression (*Figure 6C*), suggesting that Gal-3C blunted iNOS-dependent with arginase-1-alternative profibrotic responses. Moreover, Gal-3C delayed treatment reduced phospho-IKKβ and NF-κB phospho-P65 without altering phospho-IKKα and phospho-Akt levels (*Figure 6D* and *E*), indicating a regulatory role of Gal-3C in the IKKβ/NF-κB/iNOS signalling cascade of profibrotic pathways post-MI (*Figure 7A*).

3.10 Gal-3C treatment altered the phenotypic characterization of macrophages during reparative phase post-MI

Following the early inflammatory phase post-MI, the reparative phase is characterized by polarization of immune cells towards a wound-healing state. As part of this process, the population of infarct macrophages experiences a shift from M1 to M2 phenotype to resolve inflammation and promote myofibroblast proliferation and wound repair.[1] To determine if the inhibition of M2 polarization by Gal-3C treatment observed *in vitro* (*Figure 6A*) occurred physiologically, we sorted M1 and M2 macrophages from digested LV tissues from animals 14 days post-MI with Gal-3C 7-day delayed treatment to quantitate the distribution of macrophage phenotypes.

Flow cytometry was used to identify macrophages as M1 ($CD45^+CD68^+CD86^+$) and M2 ($CD45^+CD68^+CD163^+$) phenotypes

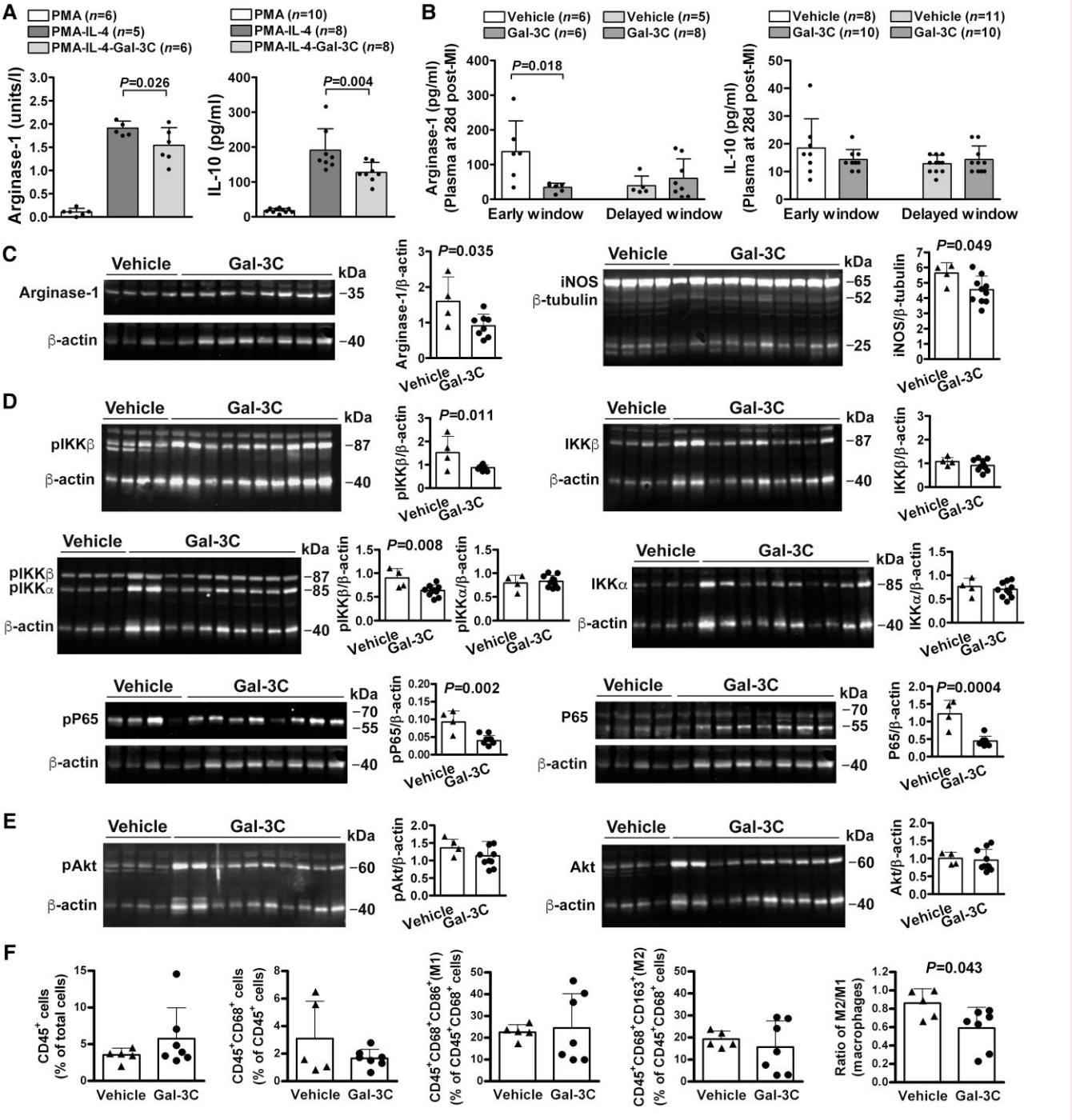

Figure 6 Gal-3C treatment reduced arginase-1 and IL-10 *in vitro*, decreased post-MI plasma arginase-1, and down-regulated myocardial iNOS through signalling of IKKβ/NF-κB along with reductions in arginase-1, and altered the phenotypic properties of infarct macrophages. (*A*) Levels of arginase-1 and IL-10 in human macrophage-like cells. Graphs illustrate the mean of 5–6 (arginase-1) and 8–10 (IL-10) biological replicates in one experiment and are each representative of three separate experiments. (*B*) Plasma levels of arginase-1 and IL-10 post-MI. One outlier was removed from vehicle delayed-window arginase-1 (973 pg/mL). (*C*) Immunoblot analyses of myocardial arginase-1 and iNOS. For iNOS, monomeric bands were detected at 65 kDa. (*D*) Myocardial expression of IKKβ, IKKα, and NF-κB P65. pIKKβ, phospho-IKKβ; pIKKα, phospho-IKKα; pP65, phospho-P65. For pIKKβ, two bands were observed in the vehicle group, whereas one band was observed in the Gal-3C group. We measured the intensity of two bands in the vehicle group for comparison. (*E*) Myocardial expression of Akt. Sample number in (*C*–*E*): vehicle, $n = 4$; Gal-3C, $n = 8$–10. (*F*) Cardiac macrophage phenotypes post-MI by flow cytometry. Bar graphs representing the percentages of $CD45^+$ cells in total cells and $CD45^+CD68^+$ cells in $CD45^+$ cells, the relative percentage of $CD45^+CD68^+CD86^+$ (M1) and $CD45^+CD68^+CD163^+$ (M2) macrophages, and the ratio of M2/M1 macrophages. Representative dot plots identifying cells are shown in Supplementary material online, *Figure S8*. Sample number: vehicle, $n = 5$; Gal-3C, $n = 7$. Statistical tests: one-way ANOVA followed by the Student–Newman–Keuls method (*A*); Student's unpaired *t*-test (*B*–*F*).

(see Supplementary material online, *Figure S8*), and analyse alterations in the relative proportions of macrophage subsets from infarcted hearts. Gal-3C delayed treatment changed the phenotypic properties of macrophages by reducing the ratio of M2/M1 macrophages compared with vehicle (*Figure 6F*), revealing reduced M2 polarization of the infarct macrophage subpopulations during reparative response following MI.

4. Discussion

Our results showed that short-term inhibition of galectin-3 with Gal-3C in the treatment of acute MI in young and aged rats limited excessive fibrosis, leading to better post-MI LV contractility, less LV dilatation, and prevention of HFrEF, along with profound benefits in EF, ESV, EDV, haemodynamics, infarct size, and interstitial fibrosis; and was more effective than standard ARB and MRA therapies.

Mechanistically, Gal-3C limited M2 polarization of macrophages as evidenced by reductions of arginase-1, IL-10, IL-6, and the ratio of infarct M2/M1 macrophages. Gal-3C impeded progressive fibrosis post-MI by averting a galectin-3-iNOS-mediated profibrotic pathway through IKKβ/NF-κB, modulating the impact of endogenous arginase-1/iNOS on the profibrotic signalling of diverse molecular mechanisms post-MI.

Galectin-3 is a key link between macrophages, fibroblasts, and the profibrotic phenotype in organ fibrosis.[5,6,8,9] The up-regulation of galectin-3 was correlated with increased levels of ECM proteins.[6,24] Exogenous galectin-3 stimulated cultured primary rat fibroblasts to proliferate and to produce collagen *in vitro,* and galectin-3 administration to healthy rats induced cardiac fibrosis and LV dysfunction.[6] Consistent with these observations, we and others have found that circulating levels of galectin-3 were increased post-MI in mice (see Supplementary material online, *Figure S1A*), rats,[14] and humans.[12] Overall, these findings indicate that galectin-3 induces collagen production, leads to fibrosis during cardiovascular disease progression, and promotes HF in rodents and humans.

Inflammation is an immediate and complex response to an MI. Subsequently, the reparative arm of the wound-healing response invokes fibrosis. Galectin-3, secreted by M2 macrophages, affects myofibroblast activation and fibrosis through TGF-β-mediated pathways by inducing alternative macrophage activation and the secretion of profibrotic cytokines that promote expansion of the fibroblast population in the injured heart.[5,8] Macrophages are the main source of arginase.[17] After injury, the arginase alternative pathway contributes to the shift of the macrophage population towards the M2 phenotype that releases arginase-1, thus playing an important role in promoting cellular proliferation and tissue fibrosis.[18,25,26] Our *in vitro* data indicated that Gal-3C inhibits M2 polarization of macrophage-like cells and reduces their profibrotic M2-phenotypic expression of arginase-1 and IL-10, which could be due to the inhibition of the positive feedback loop whereby galectin-3 induces its own secretion by M2 macrophages.[5]

Notably, the reduction of M2 polarization was evident physiologically *in vivo* by Gal-3C treatment. Early treatment reduced plasma levels of arginase-1 and IL-6, indicating the reduction of M2 polarization since IL-6 enhances M2 polarization resulting in increased arginase-1;[27] whereas delayed treatment reduced M2 polarization of infarct macrophages and expression of myocardial arginase-1, impeding M2-macrophage-arginase-1 alternative pathway that promotes pathological fibrosis post-MI.

When macrophages adapt or change their function during injury, they simultaneously co-express functional arginase-1 and iNOS depending on the state of activation/polarization, influencing signalling, proliferation, and fibrosis in different ways.[17] Accordingly, upsetting a delicate balance between arginase-1 and iNOS after an injury could functionally shift their roles. Leucocyte iNOS is vital for chronic inflammation and remodelling in MI/HF, imparting deleterious effects that accelerate HF progression post-MI.[19] Likewise, monocytes in patients with HF exhibit robust iNOS expression.[28] Moreover, IKKβ/NF-κB activation is a crucial signalling cascade for inflammatory response in inflammatory cells and in the development of HF.[29] Our results indicated that Gal-3C therapy limited post-MI fibrosis through negative regulation of the IKKβ/NF-κB/iNOS signalling cascade, implicating iNOS as a main driver of fibrosis. One mechanistic explanation for down-regulated iNOS by Gal-3C is that Gal-3C inhibits a galectin-3-M2-macrophage positive feedback loop, accordingly reducing the ongoing inflammatory reparative response that enhances inflammatory cell iNOS (*Figure 7A*). Taken together, our findings support an underlying molecular mechanism by which Gal-3C combats pathological cardiac fibrosis post-MI by inhibiting a distinct galectin-3/IKKβ/NF-κB/iNOS-driven

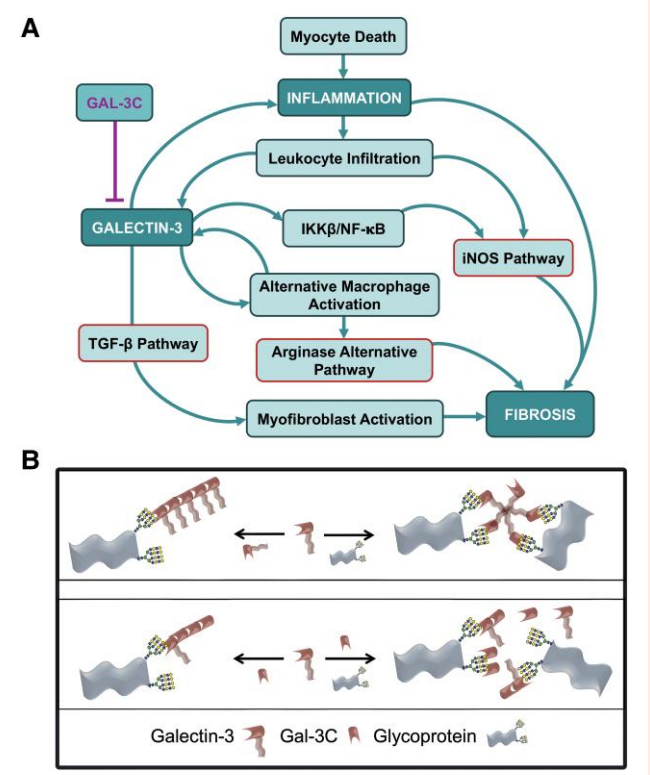

Figure 7 Illustrations of multiple roles of galectin-3 in inflammation and fibrosis and self-association and binding of galectin-3 and Gal-3C to carbohydrate ligands. (*A*) Galectin-3-associated profibrotic pathways in the infarcted myocardium. Inflammation triggered by myocyte death leads to robust infiltration into the heart of inflammatory leucocytes that release galectin-3. Increased galectin-3 contributes to myofibroblast activation through a canonical TGF-β pathway for fibrosis. Likewise, galectin-3 can affect profibrotic signalling by alternatively activating macrophages with persistent M2 phenotype involving the arginase alternative pathway, thus activating a galectin-3 positive feedback loop. Additionally, cardiac fibrosis and remodelling requires up-regulation of iNOS by galectin-3 through signalling of IKKβ/NF-κB. Notably, the inhibition of galectin-3 by Gal-3C regulates these post-MI inflammatory profibrotic signalling cascades. (*B*) The CRDs are shown with a notch for the carbohydrate-binding site. The binding of galectin-3 (top right) through its CRD to the *N*-glycans of glycoproteins can result in the formation of oligomers through non-CRD self-association of galectin-3 that causes glycoprotein clustering. Non-activating CRD self-association of galectin-3 (top left) competes with its glycoprotein binding. The binding of Gal-3C to *N*-glycans of glycoproteins (bottom right) does not result in the formation of oligomers that cause glycoprotein clustering because Gal-3C lacks the non-CRD domain present in galectin-3. CRD-mediated self-association (bottom left) occurs with Gal-3C, and occurs between Gal-3C and galectin-3. Thus, Gal-3C inhibits glycoprotein clustering induced by galectin-3 by binding to the carbohydrate ligands of galectin-3, and by binding to the CRD of galectin-3.

profibrotic pathway in conjugation with alternative arginase pathway (*Figure* 7*A*).

Our results indicate that Gal-3C therapy averted an augmentation of the fibrotic process post-MI, supporting the potential for galectin-3 inhibition as a therapeutic strategy for preventing excessive periinfarct fibrosis that progressively worsens post-MI contractile performance, leading to HFrEF. Other galectin-3 inhibitors have been investigated for therapeutic activity and produced beneficial effects in animal studies related to organ fibrosis, including carbohydrates such as *N*-acetyllactosamine,[24] multivalent polysaccharide inhibitors from plants such as modified citrus pectin (MCP)[30] and galactoarabino-rhamnogalaturonan,[31] and synthetic small molecules.[9] Some galectin-3 inhibitors have reached clinical trials for conditions including kidney, liver, and idiopathic pulmonary fibrosis. However, large molecules that present extracellular multivalent ligands for binding galectin-3 could lack efficacy. For example, administration of MCP to mice (200 mg/kg/day for 2 months followed by 500 mg/kg/day for 2 months) did not produce beneficial effects in a transgenic model of dilated cardiomyopathy/HF.[32] Furthermore, the human galectin-3 binding protein, a large circulating glycoprotein with multiple galectin-3 binding sites (*Figure* 7*B*), is a negative prognostic indicator for cancer and organ fibrosis.

Gal-3C offers potential advantages for clinical use. Consisting of the carboxy-terminal residues of human galectin-3 containing the CRD, Gal-3C binds to the galectin-3 CRD, participating in the type-C self-association of galectin-3 (*Figure* 7*B*), which is non-activating.[33,34] Gal-3C also binds to carbohydrates that are ligands for galectin-3.[35] Thus, Gal-3C uniquely acts by two distinct mechanisms to inhibit galectin-3. Gal-3C at the highest concentration (1500 μg/day) was less effective than the 600 μg/day dose, which could be due to increased Gal-3C binding to itself that would reduce its binding to galectin-3 or to the carbohydrate ligands of galectin-3.[36] Similarities in carbohydrate-binding mediated biodistribution and subcellular localization of Gal-3C and galectin-3 could be beneficial therapeutically. Radionuclide imaging of rat myocardium 4 h after injection of ^{123}I-labelled galectin-3 revealed its higher uptake into infarct compared with control hearts at 2 weeks post-injury.[37]

Galectin-3 is localized and bioactive within the cytoplasm and nucleus of cells, is secreted by non-classical mechanisms, and can be taken up by carbohydrate-dependent and independent manners.[38] Exogenous Gal-3C can also be taken up by cells in a lactose-inhibitable manner and localized in the cytoplasm and nucleus of cells.[39] Therefore, Gal-3C treatment post-MI could be beneficial by inhibiting galectin-3 both intra- and extracellularly. For clinical use, Gal-3C could be administered via intravenous infusion or subcutaneous injection.

Whereas some of the initial wound-healing fibrotic response to MI could be necessary to stabilize the infarct scar and prevent cardiac rupture, limiting fibrosis to prevent excess scar formation and infarct expansion and subsequent HFrEF is expected to improve clinical outcomes and reduce mortality secondary to HF. Infarct macrophages play important roles in the activation of inflammatory cascades and wound-healing.[40] The proinflammatory cytokine IL-6 is up-regulated early post-MI and promotes necrotic tissue resorption and wound-healing.[1,41,42] Interfering with this initial wound-healing response could be detrimental by increasing the risk of cardiac rupture. Accordingly, we measured plasma levels of IL-6 post-MI and found that unlike delayed-window treatment with Gal-3C, early-window treatment lowered circulating IL-6, indicating that treatment too soon after MI could have differential effects with some potentially detrimental. Notably, cardiac function was significantly and progressively improved by delayed treatment with Gal-3C, suggesting that improvements in chronic cardiac dysfunction were secondary to the attenuation of fibrotic responses. This is the first study to demonstrate that Gal-3C's antifibrotic effects are more beneficial than treatment with current cardiovascular drugs (losartan and spironolactone) in rodent models of MI. This study provides evidence of distinct regulatory mechanisms by which Gal-3C limits multiple fibrogenic signals, specifically iNOS and arginase-1, by targeting galectin-3. Our study included an arm in which greater efficacy was observed in treating MI in 1.5-year-old rats, equivalent to middle-aged humans. This implies a likely clinical utility of Gal-3C for elderly people with MI, which is important because MIs typically do not occur in the young, but in aged individuals. Age-related cardiac fibrosis has a major impact on the development of HF in humans.[43] Senescent hearts are prone to adverse dilative remodelling that could lead to the defects in healing and worsening HF following MI due to an impaired reparative response.[16,43] Thus, the ability to limit cardiac fibrosis and prevent adverse dilative remodelling and HF after MI in aged individuals is especially salient. Importantly, we showed that in healthy 1.5-year-old Fischer rats, comparable to middle-aged humans, Gal-3C was very effective at preserving post-MI cardiac function. Surprisingly, treatment with Gal-3C brought LVEF back to pre-MI levels in the aged Fischer rats, in contrast to the young Sprague–Dawley rats, in which treatment only partially brought LVEF back to its higher pre-MI levels. A limitation of this experiment was that, for reasons of availability, the aged rats were of the Fischer strain, whereas the young rats were of the Sprague–Dawley strain, so direct comparisons of the extent of therapeutic effect are confounded by these strain differences. Nevertheless, the fact that the antifibrotic therapy was remarkably effective in the older animals is notable and bodes well for the ultimate clinical applicability of Gal-3C.

Interstitial fibrosis eventually occurs in both HFrEF and HFpEF phenotypes, characterized by excessive ECM deposition surrounding cardiomyocytes, reducing ventricular compliance associated with progressive HF.[1] Increased galectin-3 is greatly associated with both HF phenotypes.[10] We have demonstrated that Gal-3C therapy, in both young and aged rats with MI, limited excessive interstitial fibrosis through regulating the inflammatory profibrotic cascades of galectin-3/IKKβ/NF-κB/iNOS that are linked to molecular regulatory mechanisms of HF phenotypes. This prevented subsequent LV enlargement and HFrEF following MI, indicating that therapeutic interventions using Gal-3C may provide similar beneficial effects in patients.

4.1 Limitations

This preclinical research reveals that 7-day treatment with Gal-3C provides powerful functional improvements post-MI, impeding galectin-3-mediated profibrotic progression. Particularly, Gal-3C treatment alters the phenotypic properties of infarct macrophages that play key roles in inflammation and in the remodelling and activation of other immune cells through the secretion of cytokines and chemokines.[1] Since infarct macrophages could interact with cardiomyocytes, fibroblasts, and endothelial cells, a limitation of our study is that the causal-effective relationships between Gal-3C and other cellular targets remain ambiguous. However, profibrotic signalling mediators and drivers that are active in inflammatory cells are active also in inflammatory fibroblasts and myofibroblasts during infarct healing. Thus, the mediator galectin-3 and drivers iNOS/arginase-1 could co-localize with associated cells, such as leucocytes/macrophages, fibroblasts, cardiomyocytes, and endothelial cells amid the infarcted myocardium, leading to a profibrotic milieu after MI. Overall, Gal-3C treatment reveals a distinct link between galectin-3 and iNOS/arginase-1, contributing to post-MI fibrotic progression and the development of HF.

5. Conclusions

Short-term treatment of young and aged rats with Gal-3C beginning on Day 5 post-MI remarkably improved LV pump function with attenuated dilation, and limited adverse dilative remodelling by reducing interstitial fibrosis, thereby preventing progressive HF. Our results demonstrate that Gal-3C has promising clinical potential as an emerging therapeutic agent for treatment of patients post-MI or with progressive HF.

Supplementary material

Supplementary material is available at *Cardiovascular Research* online.

Authors' contributions

M.L.S., C.M.J., and M.G. conceived the project. X.W. and H.Q. performed *in vivo* experiments and analysed data with support from M.C., L.Y., P.R.,

and P.N. M.G., K.M., B.A.C., and X.W. contributed to *in vitro* experiments and data analysis; B.A.C. and K.M. purified and analysed Gal-3C. H.J.R., S.N., R.D., and D.D.H. contributed to histological and biological analyses. X.W., M.L.S., and C.M.J. wrote the manuscript.

Acknowledgements

We thank W. Grossman for helpful discussion and advice, J.L. Delrosario, E. Luu, and M. Navabzadeh for technical assistance, and R. Zheng for help with figure preparation. We are grateful to T. Roach for help with the flow cytometry protocol, and A. Carlos, V. Nguyen, and T. Roach for data analysis, and thank the UCSF Parnassus Flow Cytometry CoLab with support grant awards (RRID:SCR_018206 and DRC Center Grant NIH P30 DK063720) for flow cytometry assistance.

Conflict of interest: C.M.J., M.G., M.L.S., and X.W. are inventors on issued and pending patents for methods and compositions for preventing and treating damage to the heart (issued: US 10369195, US 11179439; pending: EP3496738A1, CN201780062232.1A). M.G., K.M., B.A.C., and C.M.J. were employees of and have equity in MandalMed, Inc., USA. All other authors declare that they have no competing interests.

Funding

This work was supported by the National Institutes of Health (R43 HL120645 and R44 AG054386 to C.M.J. and M.L.S.).

Data availability

All data are available upon request.

References

1. Prabhu SD, Frangogiannis NG. The biological basis for cardiac repair after myocardial infarction: from inflammation to fibrosis. *Circ Res* 2016;**119**:91–112.
2. de Boer RA, De Keulenaer G, Bauersachs J, Brutsaert D, Cleland JG, Diez J, Du XJ, Ford P, Heinzel FR, Lipson KE, McDonagh T, Lopez-Andres N, Lunde IG, Lyon AR, Pollesello P, Prasad SK, Tocchetti CG, Mayr M, Sluijter JPG, Thum T, Tschope C, Zannad F, Zimmermann WH, Ruschitzka F, Filippatos G, Lindsey ML, Maack C, Heymans S. Towards better definition, quantification and treatment of fibrosis in heart failure. A scientific roadmap by the Committee of Translational Research of the Heart Failure Association (HFA) of the European Society of Cardiology. *Eur J Heart Fail* 2019;**21**:272–285.
3. Schieffer B, Wirger A, Meybrunn M, Seitz S, Holtz J, Riede UN, Drexler H. Comparative effects of chronic angiotensin-converting enzyme inhibition and angiotensin II type 1 receptor blockade on cardiac remodeling after myocardial infarction in the rat. *Circulation* 1994;**89**:2273–2282.
4. Silvestre JS, Heymes C, Oubénaïssa A, Robert V, Aupetit-Faisant B, Carayon A, Swynghedauw B, Delcayre C. Activation of cardiac aldosterone production in rat myocardial infarction: effect of angiotensin II receptor blockade and role in cardiac fibrosis. *Circulation* 1999;**99**:2694–2701.
5. MacKinnon AC, Farnworth SL, Hodkinson PS, Henderson NC, Atkinson KM, Leffler H, Nilsson UJ, Haslett C, Forbes SJ, Sethi T. Regulation of alternative macrophage activation by galectin-3. *J Immunol* 2008;**180**:2650–2658.
6. Sharma UC, Pokharel S, van Brakel TJ, van Berlo JH, Cleutjens JP, Schroen B, André S, Crijns HJ, Gabius HJ, Maessen J, Pinto YM. Galectin-3 marks activated macrophages in failure-prone hypertrophied hearts and contributes to cardiac dysfunction. *Circulation* 2004;**110**:3121–3128.
7. Calvier L, Martinez-Martinez E, Miana M, Cachofeiro V, Rousseau E, Sadaba JR, Zannad F, Rossignol P, Lopez-Andres N. The impact of galectin-3 inhibition on aldosterone-induced cardiac and renal injuries. *JACC Heart Fail* 2015;**3**:59–67.
8. Suthahar N, Meijers WC, Sillje HHW, Ho JE, Liu FT, de Boer RA. Galectin-3 activation and inhibition in heart failure and cardiovascular disease: an update. *Theranostics* 2018;**8**:593–609.
9. Mackinnon AC, Gibbons MA, Farnworth SL, Leffler H, Nilsson UJ, Delaine T, Simpson AJ, Forbes SJ, Hirani N, Gauldie J, Sethi T. Regulation of transforming growth factor-β1-driven lung fibrosis by galectin-3. *Am J Respir Crit Care Med* 2012;**185**:537–546.
10. de Boer RA, Lok DJ, Jaarsma T, van der Meer P, Voors AA, Hillege HL, van Veldhuisen DJ. Predictive value of plasma galectin-3 levels in heart failure with reduced and preserved ejection fraction. *Ann Med* 2011;**43**:60–68.
11. Asleh R, Enriquez-Sarano M, Jaffe AS, Manemann SM, Weston SA, Jiang R, Roger VL. Galectin-3 levels and outcomes after myocardial infarction: a population-based study. *J Am Coll Cardiol* 2019;**73**:2286–2295.
12. McCullough PA, Olobatoke A, Vanhecke TE. Galectin-3: a novel blood test for the evaluation and management of patients with heart failure. *Rev Cardiovasc Med* 2011;**12**:200–210.
13. John CM, Leffler H, Kahl-Knutsson B, Svensson I, Jarvis GA. Truncated galectin-3 inhibits tumor growth and metastasis in orthotopic nude mouse model of human breast cancer. *Clin Cancer Res* 2003;**9**:2374–2383.
14. Sanchez-Mas J, Lax A, Asensio-Lopez MC, Fernandez-Del Palacio MJ, Caballero L, Garrido IP, Pastor F, Januzzi JL, Pascual-Figal DA. Galectin-3 expression in cardiac remodeling after myocardial infarction. *Int J Cardiol* 2014;**172**:e98–e101.
15. Weber KT, Sun Y, Bhattacharya SK, Ahokas RA, Gerling IC. Myofibroblast-mediated mechanisms of pathological remodelling of the heart. *Nat Rev Cardiol* 2013;**10**:15–26.
16. Biernacka A, Frangogiannis NG. Aging and cardiac fibrosis. *Aging Dis* 2011;**2**:158–173.
17. Thomas AC, Mattila JT. "Of mice and men": arginine metabolism in macrophages. *Front Immunol* 2014;**5**:479.
18. Tengbom J, Cederström S, Verouhis D, Bohm F, Eriksson P, Folkersen L, Gabrielsen A, Jernberg T, Lundman P, Persson J, Saleh N, Settergren M, Sörensson P, Tratsiakovich Y, Tornvall P, Jung C, Pernow J. Arginase 1 is upregulated at admission in patients with ST-elevation myocardial infarction. *J Intern Med* 2021;**290**:1061–1070.
19. Kingery JR, Hamid T, Lewis RK, Ismahil MA, Bansal SS, Rokosh G, Townes TM, Ildstad ST, Jones SP, Prabhu SD. Leukocyte iNOS is required for inflammation and pathological remodeling in ischemic heart failure. *Basic Res Cardiol* 2017;**112**:19.
20. Takimoto Y, Aoyama T, Keyamura R, Shinoda E, Hattori R, Yui Y, Sasayama S. Differential expression of three types of nitric oxide synthase in both infarcted and non-infarcted left ventricles after myocardial infarction in the rat. *Int J Cardiol* 2000;**76**:135–145.
21. Maier HJ, Schips TG, Wietelmann A, Kruger M, Brunner C, Sauter M, Klingel K, Bottger T, Braun T, Wirth T. Cardiomyocyte-specific IκB kinase (IKK)/NF-κB activation induces reversible inflammatory cardiomyopathy and heart failure. *Proc Natl Acad Sci USA* 2012;**109**:11794–11799.
22. Mirandola L, Nguyen DD, Rahman RL, Grizzi F, Yuefei Y, Figueroa JA, Jenkins MR, Cobos E, Chiriva-Internati M. Anti-galectin-3 therapy: a new chance for multiple myeloma and ovarian cancer? *Int Rev Immunol* 2014;**33**:417–427.
23. Wang X, Takagawa J, Lam VC, Haddad DJ, Tobler DL, Mok PY, Zhang Y, Clifford BT, Pinnamaneni K, Saini SA, Su R, Bartel MJ, Sievers RE, Carbone L, Kogan S, Yeghiazarians Y, Hermiston M, Springer ML. Donor myocardial infarction impairs the therapeutic potential of bone marrow cells by an interleukin-1-mediated inflammatory response. *Sci Transl Med* 2011;**3**:100ra90.
24. Yu L, Ruifrok WP, Meissner M, Bos EM, van Goor H, Sanjabi B, van der Harst P, Pitt B, Goldstein IJ, Koerts JA, van Veldhuisen DJ, Bank RA, van Gilst WH, Silljé HH, de Boer RA. Genetic and pharmacological inhibition of galectin-3 prevents cardiac remodeling by interfering with myocardial fibrogenesis. *Circ Heart Fail* 2013;**6**:107–117.
25. Rath M, Müller I, Kropf P, Closs EI, Munder M. Metabolism via arginase or nitric oxide synthase: two competing arginine pathways in macrophages. *Front Immunol* 2014;**5**:532.
26. Kitowska K, Zakrzewicz D, Konigshoff M, Chrobak I, Grimminger F, Seeger W, Bulau P, Eickelberg O. Functional role and species-specific contribution of arginases in pulmonary fibrosis. *Am J Physiol Lung Cell Mol Physiol* 2008;**294**:L34–L45.
27. Braune J, Weyer U, Hobusch C, Mauer J, Brüning JC, Bechmann I, Gericke M. IL-6 regulates M2 polarization and local proliferation of adipose tissue macrophages in obesity. *J Immunol* 2017;**198**:2927–2934.
28. Comini L, Bachetti T, Agnoletti L, Gaia G, Curello S, Milanesi B, Volterrani M, Parrinello G, Ceconi C, Giordano A, Corti A, Ferrari R. Induction of functional inducible nitric oxide synthase in monocytes of patients with congestive heart failure. Link with tumour necrosis factor-α. *Eur Heart J* 1999;**20**:1503–1513.
29. Abe H, Tanada Y, Omiya S, Podaru MN, Murakawa T, Ito J, Shah AM, Conway SJ, Ono M, Otsu K. NF-κB activation in cardiac fibroblasts results in the recruitment of inflammatory Ly6C(hi) monocytes in pressure-overloaded hearts. *Sci Signal* 2021;**14**:eabe4932.
30. Ibarrola J, Matilla L, Martínez-Martínez E, Gueret A, Fernández-Celis A, Henry JP, Nicol L, Jaisser F, Mulder P, Ouvrard-Pascaud A, López-Andrés N. Myocardial injury after ischemia/reperfusion is attenuated by pharmacological galectin-3 inhibition. *Sci Rep* 2019;**9**:9607.
31. Chalasani N, Abdelmalek MF, Garcia-Tsao G, Vuppalanchi R, Alkhouri N, Rinella M, Noureddin M, Pyko M, Shiffman M, Sanyal A, Allgood A, Shlevin H, Horton R, Zomer E, Irish W, Goodman Z, Harrison SA, Traber PG, Belapectin Study I. Effects of belapectin, an inhibitor of galectin-3, in patients with nonalcoholic steatohepatitis with cirrhosis and portal hypertension. *Gastroenterology* 2020;**158**:1334–1345.e5.
32. Nguyen MN, Ziemann M, Kiriazis H, Su Y, Thomas Z, Lu Q, Donner DG, Zhao WB, Rafehi H, Sadoshima J, McMullen JR, El-Osta A, Du XJ. Galectin-3 deficiency ameliorates fibrosis and remodeling in dilated cardiomyopathy mice with enhanced Mst1 signaling. *Am J Physiol Heart Circ Physiol* 2019;**316**:H45–H60.
33. Lepur A, Salomonsson E, Nilsson UJ, Leffler H. Ligand induced galectin-3 protein self-association. *J Biol Chem* 2012;**287**:21751–21756.
34. Sundqvist M, Welin A, Elmwall J, Osla V, Nilsson UJ, Leffler H, Bylund J, Karlsson A. Galectin-3 type-C self-association on neutrophil surfaces; the carbohydrate recognition domain regulates cell function. *J Leukoc Biol* 2018;**103**:341–353.
35. Hsu DK, Zuberi RI, Liu FT. Biochemical and biophysical characterization of human recombinant IgE-binding protein, an S-type animal lectin. *J Biol Chem* 1992;**267**:14167–14174.
36. Ochieng J, Green B, Evans S, James O, Warfield P. Modulation of the biological functions of galectin-3 by matrix metalloproteinases. *Biochim Biophys Acta* 1998;**1379**:97–106.
37. Arias T, Petrov A, Chen J, de Haas H, Perez-Medina C, Strijkers GJ, Hajjar RJ, Fayad ZA, Fuster V, Narula J. Labeling galectin-3 for the assessment of myocardial infarction in rats. *EJNMMI Res* 2014;**4**:75.
38. Lepur A, Carlsson MC, Novak R, Dumić J, Nilsson UJ, Leffler H. Galectin-3 endocytosis by carbohydrate independent and dependent pathways in different macrophage like cell types. *Biochim Biophys Acta* 2012;**1820**:804–818.

39. Jarvis GA, Mirandola L, Cobos E, Chiriva-Internati M, John CM. Galectin-3C: human lectin for treatment of cancer. In: Klyosov AA, Traber PG (eds), *Galectins and Disease Implications for Targeted Therapeutics*. Washington, D.C.: American Chemical Society; 2012. p195–232.
40. Frantz S, Nahrendorf M. Cardiac macrophages and their role in ischaemic heart disease. *Cardiovasc Res* 2014;**102**:240–248.
41. Deten A, Volz HC, Briest W, Zimmer HG. Cardiac cytokine expression is upregulated in the acute phase after myocardial infarction. Experimental studies in rats. *Cardiovasc Res* 2002;**55**: 329–340.
42. Zhang Y, Wang JH, Zhang YY, Wang YZ, Wang J, Zhao Y, Jin XX, Xue GL, Li PH, Sun YL, Huang QH, Song XT, Zhang ZR, Gao X, Yang BF, Du ZM, Pan ZW. Deletion of interleukin-6 alleviated interstitial fibrosis in streptozotocin-induced diabetic cardiomyopathy of mice through affecting TGFbeta1 and miR-29 pathways. *Sci Rep* 2016;**6**:23010.
43. Liu CY, Liu YC, Wu C, Armstrong A, Volpe GJ, van der Geest RJ, Liu Y, Hundley WG, Gomes AS, Liu S, Nacif M, Bluemke DA, Lima JAC. Evaluation of age-related interstitial myocardial fibrosis with cardiac magnetic resonance contrast-enhanced T1 mapping: MESA (Multi-Ethnic Study of Atherosclerosis). *J Am Coll Cardiol* 2013;**62**:1280–1287.

Translational perspective

Targeting galectin-3 by Gal-3C to limit fibrosis-mediated heart failure (HF) is a promising therapy for myocardial infarction (MI). Seven-day Gal-3C therapy post-MI in young and aged rats averted HF and was more effective than two current drugs. This study provides evidence of distinct regulatory mechanisms driving profibrotic progression mediated by the inhibitor of nuclear factor (NF)-κB kinase-β (IKK-β)/NF-κB/inducible nitric oxide synthase (iNOS), by which Gal-3C could regulate multiple fibrogenic signals including arginase-1 and, thereby, limit inflammatory fibrosis in the infarcted heart. Gal-3C treatment inhibits M2-macrophage-mediated fibrosis, potentially providing a therapeutic approach to reduce morbidity and mortality in patients with MI/progressive HF.